2023 IEEE International Conference on Robotics and Automation (ICRA 2023)
May 29 - June 2, 2023. London, UK

Modeling and Inertial Parameter Estimation of Cart-like Nonholonomic Systems Using a Mobile Manipulator

Sergio Aguilera[1], Muhammad Ali Murtaza[1], Jonathan Rogers[1] and Seth Hutchinson[1]

***Abstract*— To enable a mobile manipulator to effectively maneuver a cart, we derive a dynamic model for the cart that incorporates the nonholonomic constraints on its motion, and use this model to formulate an estimator for the cart's inertial parameters. By deriving the dynamic equations of the cart using a constrained Euler-Lagrange formulation, we are able to directly incorporate nonholonomic constraints into the dynamics in a way that is independent of the kinematic parameters of the cart (e.g., specific wheel configuration, wheel radius, etc.), eliminating the need to either calibrate or estimate these kinematic parameters. We then construct an extended Kalman filter (including an explicit calculation of the linearized system and observation matrices) that uses an augmented state representation to estimate the cart's inertial parameters. We validate our approach both in simulation and experimentally using a mobile manipulator to maneuver a typical shopping cart. These experiments confirm the accuracy of our estimator, show that accurate estimation of the inertial parameters can significantly reduce the force/torque needed to successfully control the system, and illuminate the effects of varying the contact points at which the mobile manipulator applies forces and torques to guide the cart along a desired trajectory.**

I. INTRODUCTION

Mobile manipulators (MMs) are increasingly being introduced to assist humans in everyday settings, e.g., Moxi by Diligent Robotics in hospitals, a hotel luggage handling robot by Techmetics, and Hello Robot's Stretch for in-home assistance. The payload capabilities of such robots could be significantly increased with minimal design changes or additional costs if they were able to effectively maneuver passive carts, such as those shown in Fig. 1. Such carts typically have a combination of caster wheels and fixed wheels, and their inertial parameters can vary widely in different interactions (e.g. fetching an empty wheelchair and then pushing it with a patient) or as a result of discrete load changes during an interaction (e.g. loading objects into a shopping cart while moving). In these cases, because the cart's motion is affected by the MM applying forces and torques to the cart handle, it is essential to have an accurate model of the cart's dynamics, including an accurate estimation of its inertial parameters such as its mass, center of mass (COM), and moments of inertia.

Most previous research in this area has ignored the cart dynamics, either by assuming inertial parameters do not vary over time or by considering only the geometric path planning problem (which can be formulated in purely kinematic terms). A MM using a modified arm with two grippers to push a wheelchair is introduced in [8]. Their approach uses an adaptive control formulation and computes an estimate of the mass of the wheelchair. Similarly, [18] uses a MM to push a 4-caster wheels cart and performs mass estimation. In both cases, the object's CoM is considered to be known and constant, significantly simplifying the cart dynamics and estimating the cart's inertial parameters.

Fig. 1. Example of commonly used cart-like systems.

Research that considers only the geometric aspect of the problem includes [17], [14], [15], and [7], all of which focus on path planning, assuming that the MM can change the cart's orientation as needed. This assumption does not hold for heavy carts with nonholonomic constraints (e.g., non-castor wheels). Likewise, research on humanoid robots pushing heavy objects [9] and [19] focus mainly on the humanoid's posture and computing zero momentum points for the interaction between the robot and the object. A similar robot to ours is used to push/pull a pallet-jack in [1]. Using a force control for the manipulator, this system can navigate the pallet-jack to a desired configuration. However, the pallet-jack system is significantly different from a typical cart; the pallet-jack does not have caster wheels, but the orientation of the front wheels is set by the orientation of the handle, which allows to kinematically plan the cart's path.

Basic dynamic models of cart-like systems have been presented in [7], [18] and [8]. These only consider the object's mass as an important inertial parameter, and nonholonomic constraints are ignored. Differential Driven Robots (DDRs) have a similar configuration to cart-like systems, and both Euler-Lagrange and Newton-Euler methods with nonholonomic constraints have been developed in [2], [6], [11], and [12] for DDRs; however, the CoM is always considered to be known, and the control problem is formulated in terms of input wheel velocities, leading to a purely kinematic formulation of the control problem. Our dynamic model includes a richer set of inertial parameters and directly incorporates nonholonomic constraints on cart motion.

[1]Institute of Robotics and Intelligent Machines, Georgia Institute of Technology, Atlanta, GA 30332, USA sfaguile@gatech.edu

Because the inertial parameters of the cart system can vary over time (both between tasks and during individual tasks), we use an extended Kalman filter (EKF) to estimate these parameters. There has been significant research on the problem of estimating the parameters of dynamic systems, including [13], [3], [4], [16], and [5], all of which show adaptive control approaches or the use of EKF for different parameter estimations depending on the system dynamics. Our approach is most closely related to that of [20], which presents an EKF with an augmented state for parameter estimation for CoM and Mass, along other parameters of the system itself.

The contributions of this paper are as follows:

- We derive a dynamic model for cart-like systems that includes a rich set of inertial parameters, explicitly incorporates the cart's nonholonomic constraints, and is independent of the kinematic parameters of the cart.
- We propose an EKF with an augmented state considering unknown inertial parameters for parameter estimation of a passive system by applying external wrenches.
- We present both simulation and experimental results for a MM pushing a shopping cart with different inertial parameters and show successful result for mass estimation and CoM under simple trajectories.

The remainder of this paper is organized as follows. Section II presents the methodology, describing the dynamic modeling of a cart-like system, estimation of inertial parameters, and application of the control input. Simulation and experimental results are shown in section III, where we use a shopping cart as an example. Section IV presents our conclusions and future work.

II. METHODOLOGY

A. Dynamic Model of Cart-like Systems

Cart-like systems' motion is determined by their dynamic model and we must be able to predict their behavior to external forces to accurately control them. For example, a shopping cart mass can fluctuate between $15kg$ to $60kg$, and the CoM changes as we put objects on it, or a hospital bed's inertial parameters depends on the patient's mass and position. The required force needed to move the object increases with the mass, but it also dependent on the location of the CoM. E.g. To minimize the applied force of the MM at the end-effector to push a cart on a straight line, we want to apply just a linear force that goes through the CoM. Thus, we propose a simplified dynamic model for these cart-like systems using Euler-Lagrange dynamics. We consider the motion of the system in $SE(2)$ and define the following coordinate frames: spatial/world frame $\{s\}$, a fixed frame on the object $\{b\}$, and the CoM frame $\{c\}$. Since the CoM location is unknown, we will develop the Euler-Lagrange equations about frame $\{b\}$.

We consider the Lagrangian $\mathscr{L} = T - V$, where T is the kinetic energy and V is the potential energy. Since we are working in the plane, we assume that the potential energy is equal to zero. For the kinetic energy of the cart

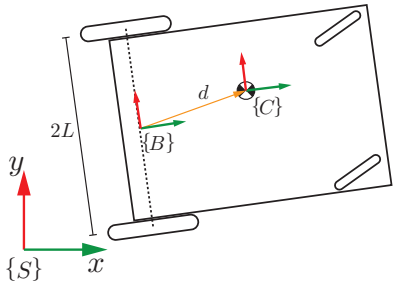

Fig. 2. Simplified cart-like system's diagram.

system, we should consider the velocity of the main body, with mass m_{cart}, and the velocity of each of the wheels rotating, with mass m_i. In general, carts either have small, light wheels that rotate fast (e.g. shopping cart) or large, heavier wheels that rotate slowly (wheelchair), therefore the kinematic energy of the wheels is negligible. Thus, we will look at the energy of the cart as a whole, with mass $m = m_{cart} + \sum m_i$, and neglect the kinetic energy contribution of the wheel's angular velocity about their axis of rotation. We define the generalized coordinates about the frame $\{b\}$ as $q^b = \begin{bmatrix} x & y & \theta \end{bmatrix}$ and the kinematic energy of the cart's CoM in the $\{b\}$ frame is given by

$$T = \frac{1}{2}m\left(\dot{x}^2 + \dot{y}^2\right) - md_x\dot{\theta}\left[\dot{x}s_\theta - \dot{y}c_\theta\right] - md_y\dot{\theta}\left[\dot{x}c_\theta + \dot{y}s_\theta\right] + \frac{1}{2}m\dot{\theta}^2\left(d_x^2 + d_y^2\right) + \frac{1}{2}I\dot{\theta}^2 \quad (1)$$

Where s_θ and c_θ are the sine and cosine functions of θ, d_x and d_y are the position of the CoM in the cart frame and I is the inertia of the system. The dynamic equations are given by

$$\frac{d}{dt}\left(\frac{\partial \mathscr{L}}{\partial \dot{q}_i}\right) - \frac{\partial \mathscr{L}}{\partial q_i} = \Gamma \quad (2)$$

where Γ are the external wrenches applied to the system. For the external wrenches, we consider three main elements, the external wrench applied by the MM, Γ_{MM}; non-conservative forces, $N(q,\dot{q})$ (e.g. viscous force as the wheels rotate); and the reaction forces introduced by the nonholonomic constraints of the wheels due to no lateral slippage. For each of the wheels, we can write the nonholonomic constraints as

$$\Lambda(q)\dot{q} = 0 \quad (3)$$

where $\Lambda(q)$ is the constraint matrix. These kinematic constraints create reactive forces that oppose any force that would create a motion along the nonholonomic constraint. Then, we can write the dynamic equations of the system as

$$M(q)\ddot{q} + C(q,\dot{q})\dot{q} = \Gamma_{MM} - N(q,\dot{q}) - \Lambda^T(q)\lambda \quad (4)$$

Where λ is a Lagrange multiplier vector (one for each linearly independent constraint) that solves for the nonholonomic constraints. Even though the caster wheels also introduce nonholonomic constraints, we assume that they quickly rotate and position along the system's direction of

motion, and we can neglect their effects. Then, our dynamic system will be given by

$$M=\begin{bmatrix} m & 0 & -m\left[d_x s_\theta + d_y c_\theta\right] \\ 0 & m & m\left[d_x c_\theta - d_y s_\theta\right] \\ -m\left[d_x s_\theta + d_y c_\theta\right] & m\left[d_x c_\theta - d_y s_\theta\right] & I + m(d_x^2 + d_y^2) \end{bmatrix}$$

$$C=\begin{bmatrix} 0 & 0 & m\dot{\theta}\left[d_y s_\theta - d_x c_\theta\right] \\ 0 & 0 & -m\dot{\theta}\left[d_y c_\theta + d_x s_\theta\right] \\ 0 & 0 & 0 \end{bmatrix} \quad \Gamma_{MM}=\begin{bmatrix} f_x \\ f_y \\ \tau \end{bmatrix} \quad N=\sigma\begin{bmatrix} \dot{x} \\ \dot{y} \\ \dot{\theta} \end{bmatrix}$$

$$\Lambda(q)=\begin{bmatrix} -\sin(\theta) & \cos(\theta) & 0 \end{bmatrix} \quad \lambda=\begin{bmatrix} \lambda_1 \end{bmatrix}$$

where σ is a positive definite, viscous coefficient that opposes the system's motion. The Lagrange multipliers add additional unknowns to the system, which can be solved by the forward dynamic of the system and then solving for the Lagrange multiplier such that the acceleration in the directions of the constraints are zero. Similarly, we can compute

$$P_\Lambda(q)=\left[I-\Lambda^T\left(\Lambda M^{-1}\Lambda^T\right)^{-1}\Lambda M^{-1}\right] \tag{5}$$

where $P_\Lambda(q)\in\mathbb{R}^{n\times n}$ is a projection matrix with rank $n-k$, and k is the number of constraints. $P_\Lambda(q)$ maps the generalized forces Γ_{MM} to $P_\Lambda\Gamma_{MM}$, which is an input force that only apply forces in the allowed directions of motion. If we multiply the constrained dynamic system by the projection matrix, we get a secondary system

$$P_\Lambda(q)\Gamma_{MM}=P_\Lambda(q)\left[M(q)\ddot{q}+C(q,\dot{q})\dot{q}+N(q,\dot{q})\right] \tag{6}$$

$$P_\Lambda(q)\Gamma_{MM}=M'(q)\ddot{q}+C'(q,\dot{q})\dot{q}+N'(q,\dot{q}) \tag{7}$$

Even though the control input is in $SE(2)$, due to the system's projection onto the unconstrained directions, the control input has only 2 degrees of freedom. So E.g. if the robot grabs the cart about the handle, we can actually just apply forces along the x-axis of the cart and torques about the z-axis, as any lateral force is dissipated by the constraints.

B. Parameter Estimation

To estimate the inertial parameters of the system, we will create an augmented state for our system. We want to estimate the mass, CoM of the system, but when studying the dynamic system, their relationships are non-linear and it's complex to decouple the effects of the CoM from the mass. Thus, we pick a set of parameters that would be linear in the dynamic equations by picking $\varphi=\begin{bmatrix} m & md_x & md_y & I+m(d_x^2+d_y^2) \end{bmatrix}^T$

For this work, an EKF is used to estimate the unknown parameters in the dynamic model. The EKF state vector consists of

$$\hat{\mathbf{x}}=\begin{bmatrix} \hat{q}^T & \dot{\hat{q}}^T & \hat{\varphi}^T \end{bmatrix}^T \tag{8}$$

where the "$\hat{}$" symbol denotes an estimate quantity. The dynamics are given by the projected system (for simplification of notation, we will omit the " $'$ " symbol for the projected matrices), $\dot{\mathbf{x}}=f(\mathbf{x}(t),u(t))$ as

$$\dot{\hat{\mathbf{x}}}=\begin{bmatrix} \dot{\hat{q}} \\ \ddot{\hat{q}} \\ \dot{\hat{\varphi}} \end{bmatrix}=\begin{bmatrix} \dot{\hat{q}} \\ \hat{M}^{-1}(\Gamma_{MM}-\hat{C}\dot{\hat{q}}-\hat{N}) \\ 0 \end{bmatrix}+\begin{bmatrix} 0 \\ 0 \\ \mu_\varphi \end{bmatrix} \tag{9}$$

where μ_φ describes the dynamics of the unknown parameters which we assume to be driven by a pure white noise process. As for the measured states of our system, we assume that all dynamic states (not the parameters) can be measure with some noise as

$$z(t)=h(\mathbf{x})=\begin{bmatrix} I_{6\times 6} & 0_{6\times 4} \end{bmatrix}\mathbf{x}+\mu_h=\begin{bmatrix} \bar{q} \\ \dot{\bar{q}} \end{bmatrix} \tag{10}$$

Where the "$\bar{}$" symbol denotes a measured quantity and μ_h is the observation noise.

We implemented a continuous-time EKF with discrete-time measurements. Due to the simplicity of the system, we can compute the analytic derivative of the dynamic system as

$$F(t)=\left.\frac{\partial f}{\partial \mathbf{x}}\right|_{\hat{\mathbf{x}}(t),u(t)} \qquad H(t)=\left.\frac{\partial h}{\partial \mathbf{x}}\right|_{\hat{\mathbf{x}}(t)} \tag{11}$$

and compute the continuous-time derivative of the system as

$$\dot{\hat{\mathbf{x}}}(t) = f(\mathbf{x}(t),u(t)) \tag{12}$$

$$\dot{P}(t) = F(t)P(t)+P(t)F(t)^T+Q(t) \tag{13}$$

where $P(t)$ is the predicted covariance estimate and $Q(t)$ is the covariance of the process noise. Then, as measurements are acquired at discrete times, we can update our predictions as

$$\hat{\mathbf{x}}_{0|0} = E\left[\mathbf{x}(t_0)\right] \tag{14}$$

$$P_{0|0} = E\left[(\mathbf{x}(t_0)-\hat{\mathbf{x}}(t_0))(\mathbf{x}(t_0)-\hat{\mathbf{x}}(t_0))^T\right] \tag{15}$$

$$\hat{\mathbf{x}}_{k|k-1} = \hat{\mathbf{x}}_{k-1|k-1}+\dot{\hat{\mathbf{x}}}(t)\Delta t \tag{16}$$

$$P_{k|k-1} = P_{k-1|k-1}+\dot{P}(t)\Delta t \tag{17}$$

Then, the update of the system computed as

$$K_k = P_{k|k-1}H_k^T\left(H_k P_{k|k-1}H_k^T+R_k\right)^{-1} \tag{18}$$

$$\hat{\mathbf{x}}_{k|k} = \hat{\mathbf{x}}_{k|k-1}+K_k\left(z_k-h(\hat{\mathbf{x}}_{k|k-1})\right) \tag{19}$$

$$P_{k|k} = (I-K_kH_k)P_{k|k-1} \tag{20}$$

where Q is the covariance of the process noise, R is the covariance of the observation noise and K is the Kalman gain.

C. Contact point and Input Wrenches

These cart-like systems are passive, and we need a MM to apply external wrenches to have them move. The dynamic modeling and parameter estimation allow us to predict and estimate the object's behavior. However, our final goal is to simplify the control and minimize the torques applied by the MM. As mentioned, when applying a wrench, forces along the nonholonomic constraints will be dissipated (or, if large enough, could have the cart flip). The MM is free to apply forces in $SE(3)$ to the object, but depending on the location of the Contact Point (CP) between the end-effector and the object, we want to satisfy a wrench that lives on the span of the projection matrix. We consider a set of contact points $\mathscr{X}$ (e.g. all points along the handle of the shopping cart), and we define the contact point frame $\{a\}$, with the same orientation as the cart's frame $\{b\}$ and origin at the CP location. Since we consider the cart as a rigid body, we can transform any

wrench at the CP to a wrench at the object's frame $\{b\}$. The MM can apply a wrench at the end-effector in task space as

$$\Gamma_{ee} = \begin{bmatrix} f_{ee} \\ \tau_{ee} \end{bmatrix} \tag{21}$$

where $f_{ee} \in \mathbb{R}^3$ and $\tau_{ee} \in \mathbb{R}^3$ are the linear forces and torques at the end-effector of the MM respectively. Even though the MM can apply a wrench in $SE(3)$, we are assuming that the cart can only move in $SE(2)$ (i.e. we will not lift or tilt the object in any direction). We will define the wrench basis for the end effector at the CP as

$$B_a = \begin{bmatrix} 1 & 0 & 0 & 0 & 0 & 0 \\ 0 & 1 & 0 & 0 & 0 & 0 \\ 0 & 0 & 0 & 0 & 0 & 1 \end{bmatrix}^T \tag{22}$$

Given a transformation $g_{ij} \in SE(3)$, defined by a transformation pair (p_{ij}, R_{ij}), which is the translation $p \in \mathbb{R}^3$ and rotation $R \in SO(3)$, between frame $\{j\}$ to frame $\{i\}$. We can transform the wrench at the end-effector to the fixed cart's frame using a grasp map, using the adjoint transformation

$$G = \left[Ad_{g_{ab}}^T B_a\right], \qquad Ad_g = \begin{bmatrix} R & [p]_\times R \\ 0 & R \end{bmatrix} \tag{23}$$

where $[p]_\times$ is the skew-symmetric matrix of the vector p. Then, we can transform between the end effector's wrench and the applied force at the CP as

$$\Gamma_{MM} = G\Gamma_{ee}. \tag{24}$$

We can look at this problem from the opposite perspective. Given a desired applied force onto the object Γ_{MM}, we can optimize over all possible contact points to minimize the force applied by the end-effector Γ_{ee}. Similarly, given multiple contact points (with multiple manipulators), we can try to minimize the effort of the manipulators by finding the minimum applied force by each manipulator that satisfies

$$\Gamma_{MM} = G_1\Gamma_{1ee} + G_2\Gamma_{2ee} + \dots \tag{25}$$

D. Persistence of Excitation

To accomplish a successful parameter estimation of a system, defining interactions or trajectories with persistence of excitation guarantees convergence without stability assumptions and ensures robustness. Regardless, as we interact with daily objects like wheelchairs, hospital beds, or shopping carts, it is not desirable to generate exciting trajectories for parameter estimation each time we need to update the parameters of our dynamic model. Instead, we would like the system to do natural trajectories, like straight-line motions along an aisle or turning, as we change the direction of motion. These simple trajectories limit the information that can be acquired but are desirable trajectories that we would expect the robot to follow when introduced into real environments.

When pushing cart-like systems, the primary goal would be to follow a trajectory or arrive at a given location with a smooth trajectory, and the parameter estimation comes as a secondary goal as we push along. Thus, during the simulation and experiments, we study the success of the parameter estimation during simple trajectories and do not use unique oscillatory acceleration profiles.

Even though we have simple trajectories, we study the introduction of the persistence of excitation by changing the contact point between the end-effector and the object.

III. SIMULATION AND EXPERIMENTAL VALIDATION

We will present and discuss the results of both simulation of a cart-like system and real hardware experiments. For example, we will use a shopping cart as our cart-like system. For both, we will discuss how relevant the dynamic model's parameters are and present the respective results. As mentioned, we are using linear trajectories or large turns to do the parameter estimation of the system, as shown in Fig. 3. All trajectories start with a step acceleration until reaching the desired speed and similarly for stopping.

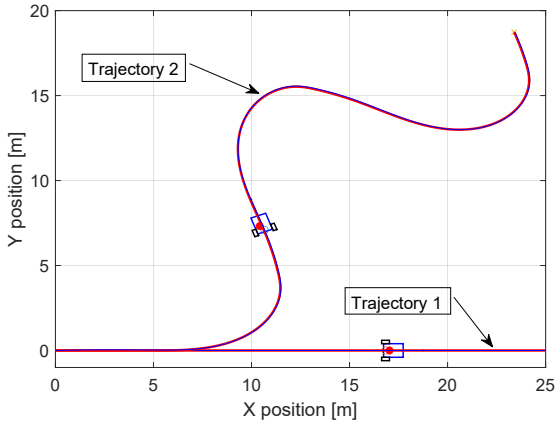

Fig. 3. Example of two trajectories. Trajectory 1 is a straight line. Trajectory 2 presents large curves along the path

A. Simulations

We are simulating our dynamic system using MATLAB. We simulate the cart being pushed by a virtual force at a CP. In the simulation, we directly control the system to follow a trajectory. Given a desired time-varying trajectory for the cart $(q_d, \dot{q}_d, \ddot{q}_d)$, we define the tracking error $e(t) = q_d(t) - q(t)$ and the auxiliary tracking error $r = \dot{e} + \alpha e$, where α is a positive definite matrix. We propose the feedback linearization

$$\Gamma_{MM} = M[\ddot{q}_d + \alpha\dot{e}] + C[\dot{q}_d + \alpha e] + N - u \tag{26}$$

and rewrite the error dynamics as

$$M\dot{r} = -Cr + u \tag{27}$$

We can define our error state space as $z(t) = \begin{bmatrix} e^T & r^T \end{bmatrix}^T$, as

$$\dot{z} = \begin{bmatrix} \dot{e} \\ \dot{r} \end{bmatrix} = \begin{bmatrix} -\alpha & I_{3\times3} \\ 0_{3\times3} & -M^{-1}C \end{bmatrix} z + \begin{bmatrix} 0_{n\times n} \\ M^{-1} \end{bmatrix} u \tag{28}$$

which is a system that we can control using a linear quadratic regulator.

TABLE I

LIST OF SIMULATION TESTS

Test	Traj.	$\hat{m}(t_0)$ [kg]	CoM [x y] [m]	noise [m]	vary CP
1	1	16	0.3 0	0.005	No
2	1	24	0.3 0	0.005	No
3	1	16	0.3 0.15	0.005	Yes
4	2	16	0.3 0	0.005	No
5	2	16	0.3 0.15	0.005	No
6	2	16	0.3 −0.15	0.005	Yes
7	2	16	0.1 0	0.005	Yes
8	2	10	0.3 0.15	0.005	No
9	2	16	0.3 0.15	0.05	Yes
10	2	16	0.3 0.15	0.2	Yes
11	2	16	0.3 0	0.005	Yes

We use this controller in simulation to be able to compare the results between controlling the system with and without parameter estimation. For the simulated environment, we performed different experiments, as shown in Table I. For the simulation, we assume a $20kg$ cart. Each experiment has one of the two desired trajectories and an initial mass estimation. For all experiments, the initial estimation of the CoM is at $(0.3m, 0m)$, but the real CoM of the simulated cart changes. Also, for each experiment, we can either have 1 constant CP at the cart or vary the CP during the interaction. For robustness, we also looked at different noise levels for the measurement in experiments 9 and 10. For the experiment 11 we incorporated discrete changes in the mass of the cart.

The tracking error results are shown in Fig. 4 for all the experiments against the same controller but without parameter estimation. For an estimation error of only $4kg$, the tracking error increases to over $20cm$ for the system with no parameter update over a couple of seconds. Even though the controller stabilizes the system at a certain distance from the tracking goal, the error is big enough that it is unreliable to move along a hallway or while rotating. For the rest of the experiments, we can see that the error diminishes quickly under $3cm$ under 5 seconds. We see an increase in error when we start rotating ($t = 7s$, $t = 16s$ and $t = 25s$), but as the location of the CoM improves, the error goes down again subsequently.

In terms of mass estimation, for all trajectories, it converges after 10 seconds, as shown in Fig. 5. When increasing

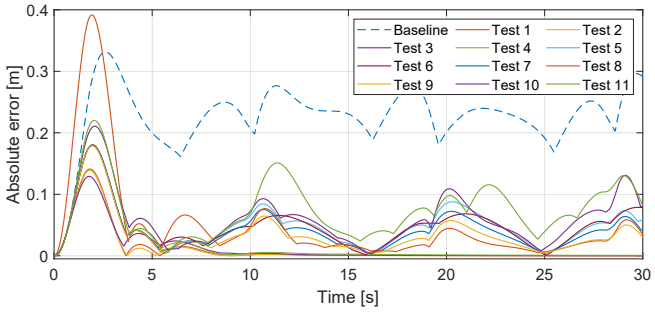

Fig. 4. Tracking error for the different Kalman filter tests.

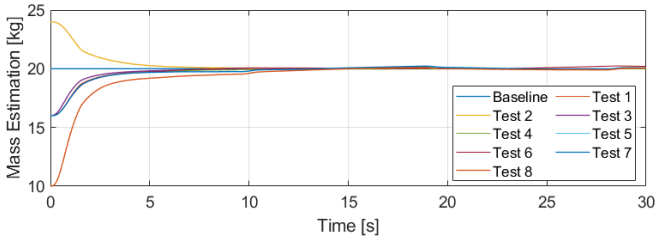

Fig. 5. Mass estimation of the tests without measurement noise.

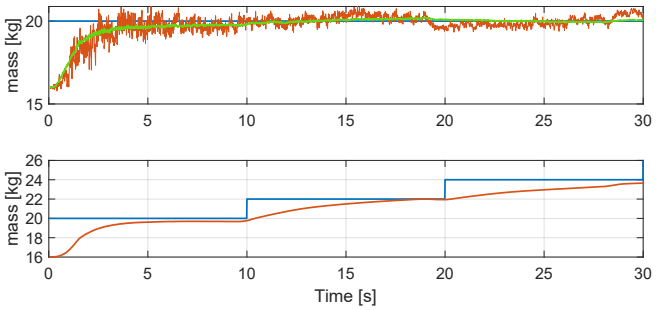

Fig. 6. Mass estimation with measurement noise of $5cm$ and $50cm$, and subject to discrete mass changes.

the noise levels of measurement and when discretely changing the cart mass as shown in Fig 6. We can also see that the EKF can correctly estimate the parameter.

We can see that the mass estimation is successful. However, the convergence is much faster when accelerating than during linear velocity segments, as seen in the change of mass experiment, which aligns with the concept of persistence of excitation. Regarding the CoM estimation, the estimation decreases the error as time progresses but did not converge after the 30 seconds interaction.

B. Experiments

For the hardware experiment, we have the setup shown in Fig. 7. The mobile manipulator is composed by a "Ridgeback" mobile base from Clearpath Robotics, an omnidirectional base that has a velocity input in $SE(2)$; a Kuka IIWA 14 manipulator, which has 7 Degrees of Freedom and a maximum payload of $14kg$; We have a "Robotiq FTS-300" Force/Torque sensor and "Robotiq 2F-85" two finger gripper. The cart is a medium shopping cart with a weight of $15kg$. To keep track of the position and velocity of the MM and the cart, we are using a Vicon camera system for motion capture. We have markers on both MM and object, and we get the position of the bodies with a $0.4mm$ mean error.

To control the system, we have the mobile base following a desired trajectory while the manipulator uses a torque controller based on Rapidly Exponentially Stabilizing Control Lyapunov functions, combined with Control Barrier Functions (to provide safety warranties), described in [10]. For this application, the torque control wants to keep the position and orientation of the manipulator relative to the mobile base. However, it has torque constraints to maintain the robot's arm out of harm. Due to the size of the space covered by

Fig. 7. Mobile Manipulator and shopping cart setup.

the Vicon system, we cannot perform the same trajectories displayed on the simulation, but we show experiments with linear trajectories ($10m$). The interaction between the MM and the cart is open-loop, the mobile base is moving in a straight line, and the end-effector is applying the required torque to keep the desired position and orientation, which then makes the cart follow a straight line. We show in the video that the controller uses just some force to keep the cart moving forward, but if the position of the contact point is too far from the CoM lateral distance, the hand does not have enough force to keep the cart moving straight.

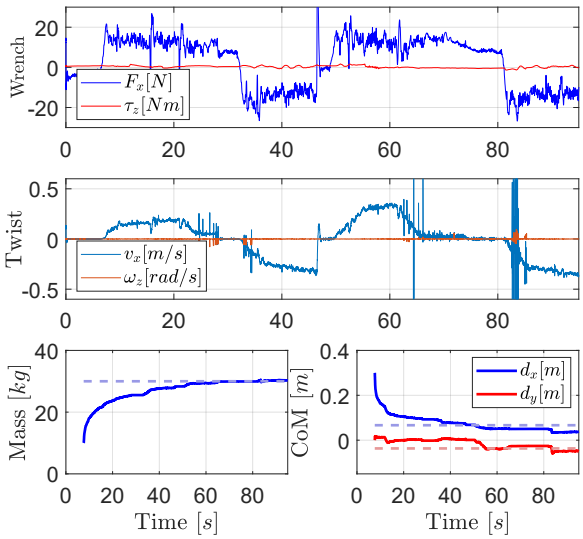

Fig. 8. Wrench profile, velocity profiles, and inertial parameter estimation for pushing a cart with a total mass of $29.7kg$.

We present the data acquired for one of the experiments in Fig. 8. The force sensor has considerable noise, with $\sim 3N$ standard deviation, while the tracking system has good position tracking but has some jumps on velocity measurements. For the estimation of the CoM, the system does not seem to converge during linear motions but jumps at moments of large force/torque measurements in the correct direction. Specifically, for the position d_y of the CoM, the EKF can determine the direction in which the CoM is, which can help us minimize the interaction force during a linear push for future control. Experiments with the shopping cart with different masses are shown in Fig. 9. For experiments $E1$ and $E5$, we show the time 4 times faster to facilitate the comparison of results. From experiments, 1 through 4 the estimation is achieved, with a low error, below $0.5kg$. The worst result is for the lightest cart ($15kg$, empty cart), which has difficulty converging due to high signal-to-noise ratios at this level of force.

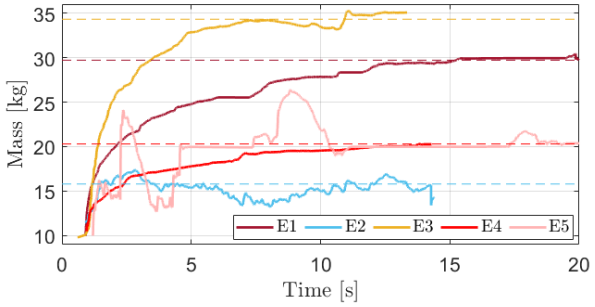

Fig. 9. Experiments on Mass estimation for cart with different payloads.

The first 4 experiments estimate parameters during linear motion, and we are not considering motion at speed under $0.05m/s$. For experiment 5, we look at not modeled systems' behaviors that can introduce noise. When changing the direction of motion from pushing to pulling, the casters wheels have to rotate in 180°, and during a short time, they oppose the change of direction due to their nonholonomic constraints (which are not modeled). When estimating during these actions, the EKF has problems, as there are additional forces that slow the velocity of the system. In each initial estimation of mass during experiment 5, there is an overestimation of the system's mass (as seen around seconds 3, 9 and 18). However, once the caster wheels align with the direction of motion, the EKF quickly converges back to the actual value.

IV. CONCLUSIONS

In this work, we have developed a dynamic model for a wide range of cart-like systems, consisting of wheels with nonholonomic constraints and not considering the system's kinematics. Even though the dynamic model is general enough, the parameter can vary widely. Thus we propose an EKF to perform state estimation for the model inertial parameters. We have shown in simulation and hardware experiments that the proposed dynamic model can be used to understand and control these systems. The proposed EKF can accurately estimate the object's mass under simple trajectories and approximate the location of the CoM that can then be used to diminish the wrench needed by the MM's end-effector. For the future work, we want to have the hardware setup controlling the system with low error and have it change the contact location to minimize the interaction forces.

V. ACKNOWLEDGMENT

Toyota Research Institute provided funds to support this work.

REFERENCES

[1] Pietro Balatti, Fabio Fusaro, Nicola Villa, Edoardo Lamon, and Arash Ajoudani. A collaborative robotic approach to autonomous pallet jack transportation and positioning. *IEEE Access*, 8:142191–142204, 2020.

[2] Alexandru Bara and Sanda Dale. Dynamic modeling and stabilization of wheeled mobile robot. In *Proceedings of the 5th WSEAS International Conference on Dynamical Systems and Control*, page 87–92, Stevens Point, Wisconsin, USA, 2009.

[3] Sayan Basu Roy, Shubhendu Bhasin, and Indra Narayan Kar. Composite adaptive control of uncertain euler-lagrange systems with parameter convergence without pe condition. *Asian J. Control*, 22(1):1–10, jan 2020.

[4] Zachary Bell, Anup Parikh, Jason Nezvadovitz, and Warren E. Dixon. Adaptive control of a surface marine craft with parameter identification using integral concurrent learning. In *2016 IEEE 55th Conference on Decision and Control (CDC)*, pages 389–394, 2016.

[5] Matt Best and T.J. Gordon. Combined state and parameter estimation of vehicle handling dynamics. 01 2000.

[6] Rached Dhaouadi and Ahmad Abu Hatab. Dynamic modelling of differential-drive mobile robots using lagrange and newton-euler methodologies: A unified framework. In *ICRA 2013*, 2013.

[7] Tekin Mericli, Manuela Veloso, and H. Levent Akin. Push-manipulation of complex passive mobile objects using experimentally acquired motion models. *Autonomous Robots*, 38, 03 2014.

[8] Nandagopal S. Methil and Ranjan Mukherjee. Pushing and steering wheelchairs using a holonomic mobile robot with a single arm. In *2006 IEEE/RSJ International Conference on Intelligent Robots and Systems*, pages 5781–5785, 2006.

[9] Masaki Murooka, Shunichi Nozawa, Yohei Kakiuchi, Kei Okada, and Masayuki Inaba. Whole-body pushing manipulation with contact posture planning of large and heavy object for humanoid robot. In *2015 IEEE International Conference on Robotics and Automation (ICRA)*, pages 5682–5689, 2015.

[10] Muhammad Ali Murtaza, Sergio Aguilera, Muhammad Waqas, and Seth Hutchinson. Safety compliant control for robotic manipulator with task and input constraints. *IEEE Robotics and Automation Letters*, 7(4):10659–10664, 2022.

[11] Aradhana Nayak, Rodrigo Sato Martín de Almagro, Leonardo Colombo, and David Martín de Diego. Optimal trajectory tracking of nonholonomic mechanical systems: a geometric approach. In *2019 American Control Conference (ACC)*, pages 1924–1929, 2019.

[12] Siti Nurmaini and Chusniah. Differential drive mobile robot control using variable fuzzy universe of discourse. In *2017 International Conference on Electrical Engineering and Computer Science (ICECOS)*, pages 50–55, 2017.

[13] Anup Parikh, Rushikesh Kamalapurkar, and Warren Dixon. Integral concurrent learning: Adaptive control with parameter convergence using finite excitation. *International Journal of Adaptive Control and Signal Processing*, 33, 10 2018.

[14] Yoonseok Pyo, Kouhei Nakashima, Tokuo Tsuji, Ryo Kurazume, and Ken'ichi Morooka. Motion planning for fetch-and-give task using wagon and service robot. In *2015 IEEE International Conference on Advanced Intelligent Mechatronics (AIM)*, pages 925–932, 2015.

[15] Antoine Rioux and Wael Suleiman. Humanoid navigation and heavy load transportation in a cluttered environment. In *2015 IEEE/RSJ International Conference on Intelligent Robots and Systems (IROS)*, pages 2180–2186, 2015.

[16] José Guadalupe Romero, Romeo Ortega, and Alexey A. Bobtsov. Parameter estimation and adaptive control of euler-lagrange systems using the power balance equation parameterization. *International Journal of Control*, 2021.

[17] Jonathan Scholz, Sachin Chitta, Bhaskara Marthi, and Maxim Likhachev. Cart pushing with a mobile manipulation system: Towards navigation with moveable objects. In *2011 IEEE International Conference on Robotics and Automation*, pages 6115–6120, 2011.

[18] Yu Sun, Ning Xi, Jindong Tan, and Yuechao Wang. Interactive model identification for nonholonomic cart pushed by a mobile manipulator. In *Proceedings 2002 IEEE International Conference on Robotics and Automation (Cat. No.02CH37292)*, volume 4, pages 3966–3971 vol.4, 2002.

[19] Jean Chagas Vaz and Paul Oh. Material handling by humanoid robot while pushing carts using a walking pattern based on capture point. In *2020 IEEE International Conference on Robotics and Automation (ICRA)*, pages 9796–9801, 2020.

[20] Kevin Webb and Jonathan Rogers. Adaptive control design for multi-uav cooperative lift systems. *Journal of Aircraft*, 58:1302–1322, 2021.